Active Sites in a Heterogeneous Organometallic Catalyst for the Polymerization of Ethylene

Culver, Damien B.; Dorn, Rick W.; Venkatesh, Amrit; Meeprasert, Jittima; Rossini, Aaron J.; Pidko, Evgeny A.; Lipton, Andrew S.; Lief, Graham R.; Conley, Matthew P.

DOI
10.1021/acscentsci.1c00466

Publication date
2021

Document Version
Final published version

Published in
ACS Central Science

ACS central science

http://pubs.acs.org/journal/acscii

Research Article

Active Sites in a Heterogeneous Organometallic Catalyst for the Polymerization of Ethylene

Damien B. Culver, Rick W. Dorn, Amrit Venkatesh, Jittima Meeprasert, Aaron J. Rossini, Evgeny A. Pidko, Andrew S. Lipton, Graham R. Lief,* and Matthew P. Conley*

Cite This: *ACS Cent. Sci.* 2021, 7, 1225–1231

Read Online

ACCESS | Metrics & More | Article Recommendations | Supporting Information

ABSTRACT: Heterogeneous derivatives of catalysts discovered by Ziegler and Natta are important for the industrial production of polyolefin plastics. However, the interaction between precatalysts, alkylaluminum activators, and oxide supports to form catalytically active materials is poorly understood. This is in contrast to homogeneous or model heterogeneous catalysts that contain resolved molecular structures that relate to activity and selectivity in polymerization reactions. This study describes the reactivity of triisobutylaluminum with high surface area aluminum oxide and a zirconocene precatalyst. Triisobutylaluminum reacts with the zirconocene precatalyst to form hydrides and passivates −OH sites on the alumina surface. The combination of passivated alumina and zirconium hydrides formed in this mixture generates ion pairs that polymerize ethylene.

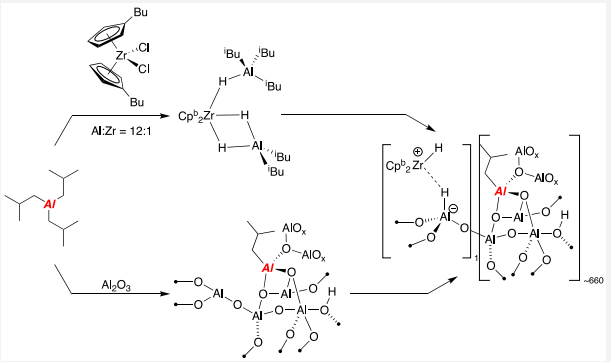

INTRODUCTION

Ziegler and co-workers discovered that mixtures of triethylaluminum and zirconium acetylacetonate polymerize ethylene to high-density polyethylene under mild conditions in 1953, and two years later Natta reported that $TiCl_4$ and Et_2AlCl mixtures polymerize propylene to stereoregular products (Figure 1a).[1,2] Derivatives from these initial discoveries evolved to heterogeneous catalysts used industrially that account for a majority of the polypropylene (PP, ∼50 millions tons) and polyethylene (PE, ∼100 million tons) produced per year. A key question related to the initial Ziegler−Natta solution catalysts was how the metal and the activator interact to form active organometallic species for polymerization reactions. This question becomes more difficult to address considering that most Ziegler−Natta catalysts are significantly more active when supported on $MgCl_2$.[3] Reactions of Cp_2TiCl_2 (Cp = cyclopentadienyl) with Et_2AlCl provided preliminary evidence for the formation of ionized organometallic active species in polymerization reactions.[4] Cp_2TiCl_2/Et_2AlCl mixtures are not particularly active in polymerization, but the serendipitous discovery of methaluminoxane (MAO) activators resulted in soluble metallocene catalysts that have activities approaching those of heterogeneous Ziegler−Natta catalysts.[5] The isolation of reactive $Cp_2ZrMe(THF)^+$ established that cationic organometallic zirconium species are active in polymerization reactions,[6] and the design of efficient activators to form cationic organometallics led to general strategies that allowed for explicit molecular design of the active site in polymerization reactions (Figure 1b).[7,8] These activators play important roles in generating catalysts that regulate molecular weight properties of the polymer and in copolymerization reactions in solution.[9−11]

Strategies to form cationic organometallic species on heterogeneous supports, the more important industrial class of catalysts for polymerization reactions, usually involve formulations containing a high surface area oxide, an excess of alkylaluminum (or MAO), and a metallocene precatalyst (Figure 1c).[12,13] Complications arising from the low quantity of active sites present in these catalysts prevent a detailed structural understanding of the active site. However, complementary studies of organometallics supported on oxides, which are likely important in these heterogeneous catalysts, arrived at similar conclusions as studies in solution. Tetraalkyl zirconium complexes supported on silica have low activity in polymerization reactions, but alumina supports provide much higher activities.[14,15] The origin of this support effect was not clear until solid-state NMR studies showed that $Cp^*_2ThMe_2$ (Cp^* = pentamethylcyclopentadienyl) reacts with Al_2O_3 to form $[Cp^*_2ThMe][Me\text{-}AlO_x]$ ion pairs,[16,17] which

Received: April 16, 2021
Published: July 13, 2021

https://doi.org/10.1021/acscentsci.1c00466
ACS Cent. Sci. 2021, 7, 1225−1231

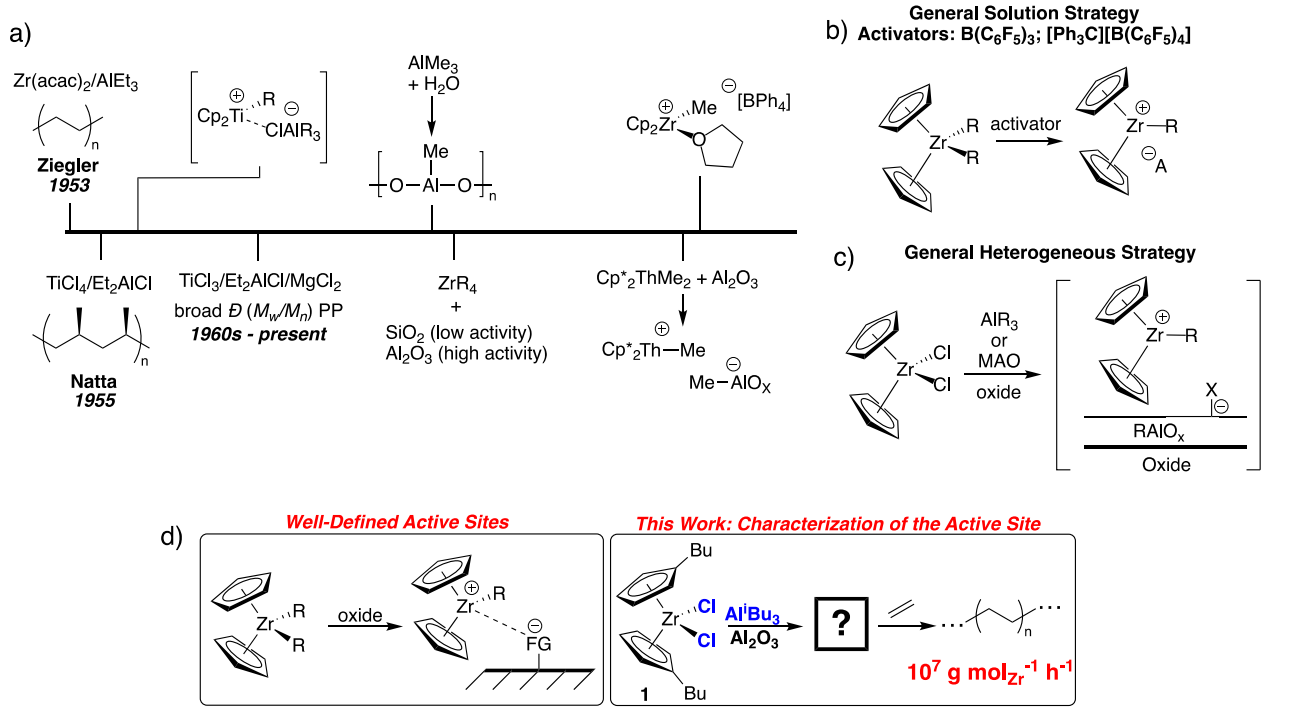

Figure 1. Evolution in the understanding of the Ziegler–Natta catalyst for olefin polymerization, showing key discoveries for homogeneous (top) and heterogeneous (bottom) catalysts (a). Current strategy to activate metallocenes in solution (b). Current strategy used industrially to form activated metallocenes on surfaces (c). Formation of well-defined sites on oxides with preformed organometallics, and the objective of this study to determine the active site structure in a model industrial catalyst for polymerization of ethylene (d).

also occurs in reactions of organozirconium complexes supported on Al_2O_3 or SiO_2/Al_2O_3.[18] This model suggests that preformed organometallics interact with an appropriate oxide to form electrophilic ion pairs that are active in polymerization reactions, a strategy employed by several groups to understand these catalysts (Figure 1d).[19−23] Though compelling, these model systems differ significantly from heterogeneous catalysts used for most industrial applications because they are derived from precatalysts containing preformed M−R groups and do not contain a large excess of alkylaluminum required in commercial polymerization reactions with metallocene chloride precatalysts.

This study describes the generation and characterization of the catalytically active sites in a ternary 1,1′-dibutylzirconocene dichloride ($(Cp^b)_2ZrCl_2$, **1**)/triisobutylaluminum (Al^iBu_3)/Al_2O_3 catalyst for the polymerization of ethylene (Figure 1d).[24,25] This mixture is complex and results in a network of reactions in solution and on the surface of Al_2O_3 to ultimately form catalytically active $[(Cp^b)_2Zr\text{-}H][H\text{-}AlO_x]$ ion pairs on the Al^iBu_3-passivated Al_2O_3 surface. The formation of ion pairs relates this catalytic mixture to the solution organometallic catalysts and well-defined heterogeneous catalysts shown in Figure 1.

RESULTS AND DISCUSSION

A mixture of **1**, Al^iBu_3, and Al_2O_3 at a Zr/Al molar ratio of 1:12 ([Zr] = 150 μmol $g_{Al_2O_3}^{-1}$) is very active in ethylene polymerization (8.4×10^7 g_{PE} mol_{Zr}^{-1} h^{-1}) and produces a modestly narrow distribution of high molecular weight PE (M_n = 90.8 kg mol^{-1}; $Đ = M_w/M_n = 4.25$). ICP-OES analysis of the isolated solid catalyst after washing shows that only 0.65 μmol of Zr g_{cat}^{-1} is present, indicating that most of the metallocene does not adsorb to the alumina surface. Omitting **1**, Al^iBu_3, or Al_2O_3 from the reaction mixture results in negligible polymerization activity (see the Supporting Information).

Al^iBu_3 and Al_2O_3 are expected to form a complex mixture of hydrolyzed alkylaluminum species bound to the Al_2O_3 surface,[26] some of which may activate **1** similar to MAO in solution. The reaction of Al_2O_3 calcined at 600 °C (~3 −OH nm^{-2}, 0.93 mmol −OH $g_{Al_2O_3}^{-1}$) with excess Al^iBu_3 in pentane forms 0.86 mmol of isobutane $g_{Al_2O_3}^{-1}$ indicating that most of the −OH groups on alumina react with Al^iBu_3. Isobutene (0.19 mmol $g_{Al_2O_3}^{-1}$) and HAl^iBu_2 also form in this reaction.

The ^{13}C cross-polarization magic angle spinning NMR (CPMAS) spectrum of Al^iBu_3/Al_2O_3 contains signals at 26 and 18 ppm for the Al−^{i}Bu fragment (Figure S7). $^1H-^{27}Al$ dipolar recoupled insensitive nuclei enhancement polarization transfer (D-RINEPT) experiments recorded under fast MAS (ν_r = 50 kHz) show that ^1H NMR signals from the Al−^{i}Bu fragment are near Al(IV) and Al(VI) sites on the Al_2O_3 surface (see the Supporting Information for details). This result is consistent with a high coverage of Al−^{i}Bu groups on the Al_2O_3 surface. DFT studies of a hydrated (110) Al_2O_3 surface containing 3 −OH nm^{-2} show exergonic adsorption and grafting of Al^iBu_3 onto the surface to form tetrahedral $(\equiv AlO)_2Al^iBu(O\text{-}(AlO_x)_2)$ shown in Figure 2a (see Supporting Information for details). Though a distribution of tetrahedral $(\equiv AlO)_2Al^iBu(O(AlO_x)_2)$ is likely present on the alumina surface, the structure of these sites has little influence on catalysis because **1** reacts with Al^iBu_3/Al_2O_3 to form inactive polymerization catalysts, showing that MAO-type sites are not present on Al^iBu_3/Al_2O_3.

Al^iBu_3/Al_2O_3 is clearly not involved in the activation of **1** but is undoubtedly relevant to formation of active sites in this catalyst. Polymerization activity is recovered when $Al^iBu_3/$

https://doi.org/10.1021/acscentsci.1c00466
ACS Cent. Sci. 2021, 7, 1225−1231

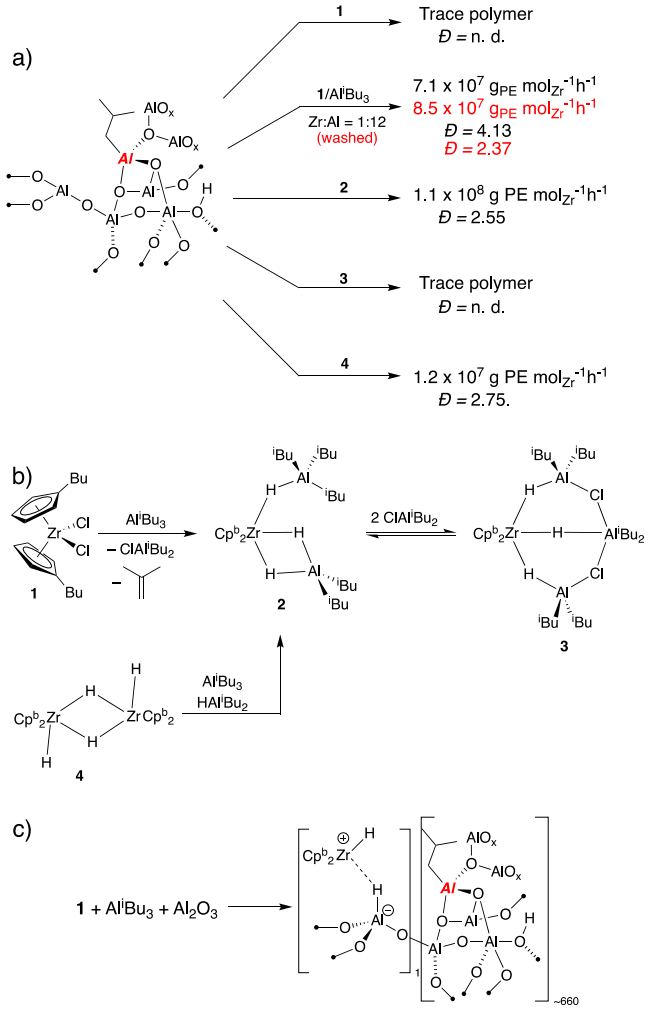

Figure 2. Polymerization activity of $(\equiv AlO)_2Al^iBu(O(AlO_x)_2)$, formed from the reaction of Al^iBu_3 with Al_2O_3, with **1** or products of the reaction of **1** and excess Al^iBu_3 (a). The aluminum originating from the Al^iBu_3 is shown in red. Products formed in the reaction of **1** with excess Al^iBu_3 and the independent synthesis of **2**, the major product in this reaction mixture (b). Generation of $[Cp^bZr\text{-}H][H\text{-}AlO_x/Al^iBu_3]$ that is consistent with polymerization activity data (c).

Al_2O_3 is contacted with a mixture of **1** and Al^iBu_3 (Zr/Al = 1:12). Removal of excess Al^iBu_3 from the solid catalyst prior to polymerization results in a catalyst that produces narrow molecular weight distributions of polymer ($Đ$ = 2.37; Figure 2a) close to the expected value characteristic of single-site behavior ($Đ$ = 2).

Under typical polymerization conditions, Al^iBu_3 is present at sufficient excess to fully saturate the Al_2O_3 surface and react with **1**. Indeed, the reaction of **1** with 12 equiv of Al^iBu_3 in deuterated methylcyclohexane (C_7D_{14}) at typical concentrations for polymerization reactions forms a mixture of isobutene, $ClAl^iBu_2$, HAl^iBu_2, $Cp^b_2Zr(\mu\text{-}H)_3(Al^iBu_2)(Al^iBu_3)$ (**2**), and $Cp^b_2Zr(\mu\text{-}H)_3(Al^iBu_2)_3(\mu\text{-}Cl)_2$ (**3**, Figure 2b). The ^{1}H NMR spectrum of this mixture at −40 °C (**2**:**3** ≈ 4:1) contains Zr−H signals at −0.98, −1.32, and −1.72 ppm for **2** as well as the Zr−H signals for **3**, which was previously reported.[27] **2** can be independently generated by mixing $[Cp^bZrH_2]_2$ (**4**) with equimolar Al^iBu_3 and HAl^iBu_2.

The formation of **2** involves Zr−Cl for Al−^{i}Bu exchange to form $ClAl^iBu_2$ and Zr−^{i}Bu intermediates that undergo β-H elimination to form Zr−H species and isobutene. Reactions of Zr−H with Al−Cl regenerate Zr−Cl and form HAl^iBu_2 that is needed to form **2** and **3**. The large excess of Al^iBu_3 facilitates exhaustive exchange with the metallocene to ultimately form $Cp^b_2ZrH_2$, which is trapped by HAl^iBu_3 and Al^iBu_3 to form **2**.

Figure 2a summarizes the polymerization activity of **2**, **3**, or **4** in the presence of Al^iBu_3/Al_2O_3. **2** reacts with Al^iBu_3/Al_2O_3 to form active polymerization catalysts with similar activities and polymer properties as *in situ* catalysts, but **3** does not form active polymerization catalysts when contacted with Al^iBu_3/Al_2O_3, showing that the alkylaluminum activator can dramatically affect polymerization productivities. **4** also reacts with Al^iBu_3/Al_2O_3 to form an active polymerization catalyst (1.2×10^7 g PE mol_{Zr}^{-1} h^{-1}; $Đ$ = 2.75). The slightly lower activity of $\mathbf{4}/Al^iBu_3/Al_2O_3$ is probably related to the higher Zr loading in this material (7.6 μmol Zr g_{cat}^{-1}), which is beneficial for mechanistic studies. This collection of data indicates that Al^iBu_3 reacts with **1** to form **2**, which is activated by Al^iBu_3/Al_2O_3 to form the ionized $[Cp^b_2Zr\text{-}H][H\text{-}AlO_x/Al^iBu_3]$ shown in Figure 2C.

$[Cp^b_2Zr\text{-}H]^+$ sites in $\mathbf{4}/Al^iBu_3/Al_2O_3$ are expected to insert vinyl halides and undergo fast β-halide elimination to form unreactive $[Cp^b_2Zr\text{-}X]^+$.[28,29] Quantification of the products in this reaction correlates with the amount of zirconium sites capable of olefin insertion. The reaction of $\mathbf{4}\text{-}d_2/Al^iBu_3/Al_2O_3$ (62% Zr−D) with excess *cis*-dichloroethylene forms *cis*/*trans*-vinyl chloride-d_1, vinyl chloride, isobutene, and a small amount of ethylene (Figure 3a). An excerpt of the ^{1}H NMR spectrum of this reaction mixture is shown in Figure 3b. On the basis of the ^{1}H NMR peak integrals, 1.8 μmol g^{-1} of vinyl chloride-d_1 form in this reaction, indicating that 23% of Zr-D$^+$ present in $\mathbf{4}\text{-}d_2/Al^iBu_3/Al_2O_3$ are active in olefin insertion reactions; this value is higher than suspected for heterogeneous polymerization catalysts formed in the presence of alkylaluminum activators but significantly lower than the active site counts for cationic metallocenes in solution.[30]

The unlabeled products probably form by the successive reactions of Zr−D$^+$ with *cis*-dichloroethylene shown in Figure 3c. Following β-chloride elimination, the surface-bound Zr−Cl$^+$ (~0.02 nm^{-2}) is alkylated by a nearby Al−^{i}Bu (~3 nm^{-2}) that regenerates a Zr−H$^+$ and forms isobutene. Subsequent reaction of Zr−H$^+$ and *cis*-dichloroethylene results in the formation of vinyl chloride and Zr−Cl$^+$. This scenario is consistent with the 1:1 ratio of isobutene: vinyl chloride-d_0 obtained from the ^{1}H NMR spectrum in Figure 3b.

Deuterium is an NMR-active quadrupolar isotope (spin I = 1). Solid-state ^{2}H NMR spectra show characteristic broad powder patterns that are a result of interactions between the nuclear electric quadrupole moment, eQ, and the electric field gradient (EFG) tensor $\boldsymbol{V}$, eq 1. The line shape of a ^{2}H MAS NMR spectrum at the slow exchange limit is described by the quadrupolar coupling constant (C_Q, eq 2) and the asymmetry parameter (η, eq 3). Terminal M−D are expected to have η = 0, bridging M−D−M that deviate from linearity is expected to have $\eta \neq 0$, and C_Q is expected to increase as the effective nuclear charge increases.[31] Thus, ^{2}H MAS NMR is capable of distinguishing between a variety of possible Zr−D structures in $\mathbf{4}\text{-}d_2/Al^iBu_3/Al_2O_3$.

$$\boldsymbol{V} = \begin{vmatrix} V_{11} & 0 & 0 \\ 0 & V_{22} & 0 \\ 0 & 0 & V_{33} \end{vmatrix} \quad (1)$$

https://doi.org/10.1021/acscentsci.1c00466
ACS Cent. Sci. 2021, 7, 1225−1231

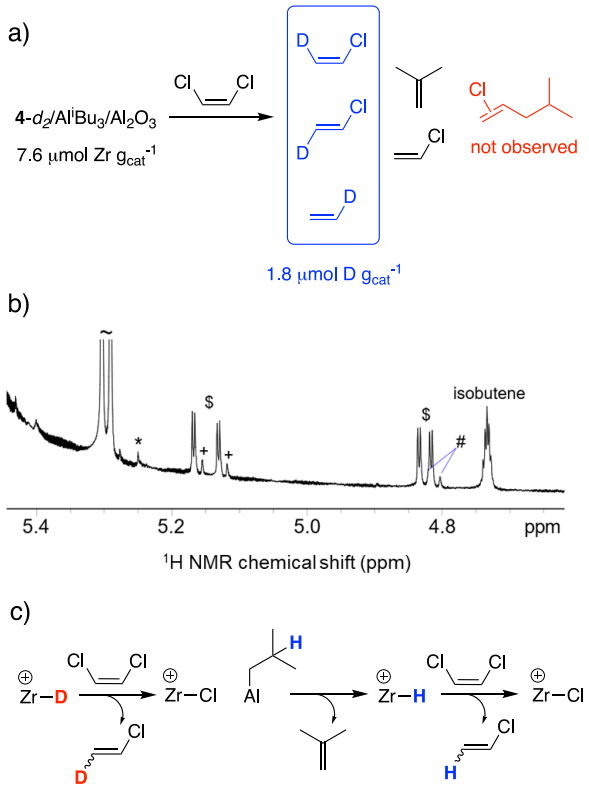

Figure 3. Reaction of 4-d_2/Al^{i}Bu$_3$/Al$_2$O$_3$ with *cis*-dichloroethylene to form reaction products (a). Excerpt of the ^{1}H NMR spectrum from 4.6−5.4 ppm (b). The symbols above each signal in (b) correspond to ~ = ^{13}C satellite from *cis*-dichloroethylene; * = ethylene; $ = vinyl chloride; + = *trans*-vinyl chloride-d_1; # = *cis*-vinyl chloride-d_1. Proposed mechanism that accounts for formation of vinyl chloride-d_1 and vinyl chloride-d_0 (c).

$$C_Q = \frac{e^2 Q V_{33}}{h} \quad (2)$$

$$\eta = \frac{V_{11} - V_{22}}{V_{33}} \quad (3)$$

Figure 4 shows ^{2}H MAS NMR spectra for 4-d_2, monomeric $(C_5Me_5)_2ZrD_2$,[32−34] $[(C_5Me_5)_2ZrD][DB(C_6F_5)_3]$,[35] and 4-$d_2$/Al^{i}Bu$_3$/Al$_2O_3$. The C_Q and η values extracted from this data are consistent with the expectations mentioned above. The ^{2}H MAS NMR spectrum of 4-d_2 is shown in Figure 4a and contains two sets of peaks assigned to the terminal Zr−D at 5.3 ppm with a C_Q of 50 kHz and η = 0, and the bridging Zr−D−Zr at −3.3 ppm with a C_Q of 44 kHz and η = 0.3, close to values reported for $[Cp_2ZrD_2]_2$.[36] The magnitude of C_Q for the Zr−D in $(C_5Me_5)_2ZrD_2$ (C_Q = 44; η = 0, Figure 4b) is similar to 4-d_2, indicating that neutral Zr−D are characterized by small C_Q values. The ^{2}H MAS NMR spectrum of $[(C_5Me_5)_2Zr-D][DB(C_6F_5)_3]$, shown in Figure 4c, contains a signal for the Zr−D$^+$ at 9.3 ppm with a C_Q of 111 kHz (η = 0) and a signal at 0.7 ppm (C_Q = 105; η = 0) for the D−B$(C_6F_5)_3$. Both $(C_5Me_5)_2ZrD_2$ and $[(C_5Me_5)_2ZrD][DB(C_6F_5)_3]$ also contain a sharp signal with a narrow $C_Q \approx$ 20 kHz for sp^3 C−D bonds that are under fast rotational exchange on the ^{2}H NMR time scale, indicating that some deuterium is incorporated into the C_5Me_5 ligand.[37]

The ^{2}H MAS NMR spectrum of 4-d_2/Al^{i}Bu$_3$/Al$_2$O$_3$ obtained at 18.8 T at 15 kHz spinning and −20 °C is shown in Figure 4d. This spectrum contains signals at 2.0 and 7.5 ppm. The signal at 2.0 ppm (C_Q = 32 kHz, η= 0.2) is also present in Al^{i}Bu$_3$/Al$_2$O$_3$ and is assigned to the natural abundance ^{2}H signal from Al^{i}Bu$_3$/Al$_2$O$_3$, but could also be a result of H/D exchange between 4 and Al−^{i}Bu groups that occurs in the synthesis of 4-d_2/Al^{i}Bu$_3$/Al$_2$O$_3$. The signal at 7.5 ppm has C_Q of 129 kHz and η of 0.35 is suggestive of a bridging Zr−D$^+$ site and supports the formation of $[Cp^b_2Zr-D][D-AlO_x]$ as the active species in 4-d_2/Al^{i}Bu$_3$/Al$_2$O$_3$. However, the signal for the $[D-AlO_x]$ site is not present in the spectrum in Figure 4d. An expansion of the ^{2}H MAS spectrum recorded at −20 °C and −100 °C is shown in Figure 4e. The spectrum at −100 °C contains a signal at 1.9 ppm for the surface Al^{i}Bu$_3$/Al$_2$O$_3$ (C_Q = 30 kHz, η = 0.3), which is slightly broader than the signal

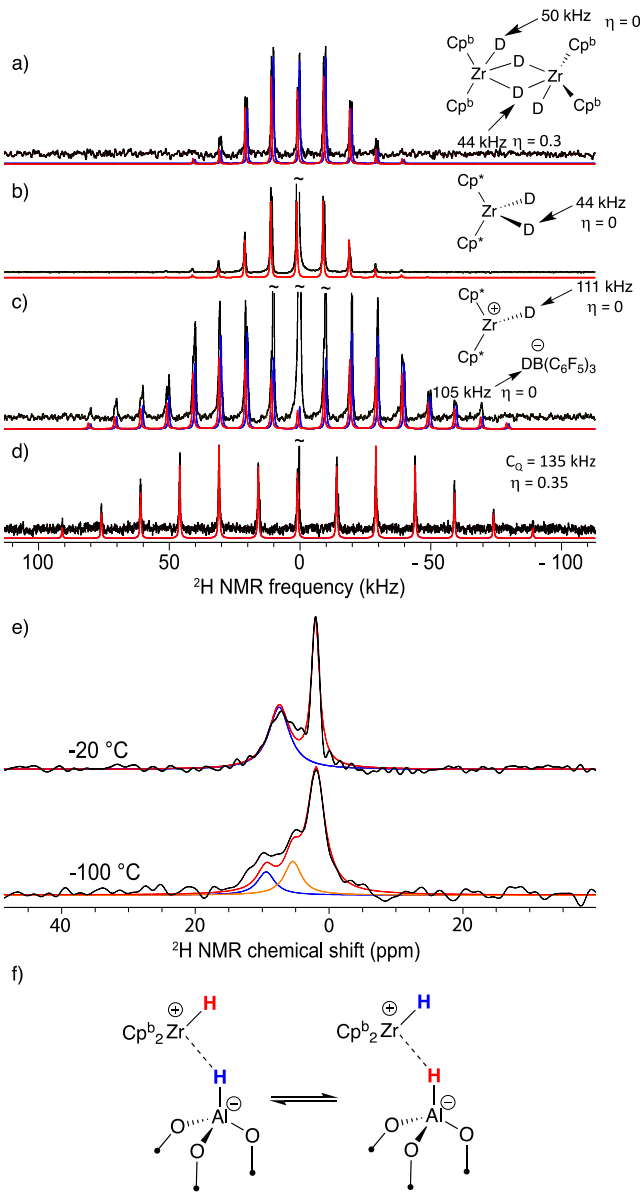

Figure 4. ^{2}H MAS NMR spectrum of dimeric $[Cp^b_2ZrD_2]_2$ (a), monomeric $Cp^*_2ZrD_2$ (b), $[Cp^*ZrD][DB(C_6F_5)_3]$ (c), and 4-d_2/Al^{i}Bu$_3$/Al$_2$O$_3$ recorded at −20 °C (d). Expansion of the ^{2}H MAS NMR spectrum from 45 to −40 ppm of 4-d_2/Al^{i}Bu$_3$/Al$_2$O$_3$ recorded at −20 °C (top) and −100 °C (e). Experimental spectra are shown in black, and simulations are shown in red, blue, or orange. Zr−H/H−Al exchange consistent with the ^{2}H MAS NMR data (f).

https://doi.org/10.1021/acscentsci.1c00466
ACS Cent. Sci. 2021, 7, 1225−1231

recorded at −20 °C. This spectrum also contains signals at 9.3 ppm (C_Q = 150 kHz, η = 0), similar to the chemical shift of the Zr−D$^+$ in $[(C_5Me_5)_2Zr{-}D]^+$ and assigned to the terminal Zr−D$^+$ of the cationic $[Cp^b{}_2Zr{-}D]^+$ fragment in 4-d_2/Al^{i}Bu$_3$/Al_2O_3, and 5.3 ppm (C_Q = 100 kHz, η = 0.5) assigned to the anionic [D−AlO$_x$] fragment in 4-d_2/Al^{i}Bu$_3$/Al_2O_3.

These results are consistent with the exchange process shown in Figure 4f. At −20 °C, the ^{2}H NMR signals for $[Cp^b{}_2Zr{-}D][D{-}AlO_x]$ undergo site exchange that results in average chemical shifts, reduced C_Q, and perturbed η values that depend on the motion these two sites, which accounts for the observation of only one ^{2}H NMR signal in 4-d_2/Al^{i}Bu$_3$/Al_2O_3 at −20 °C. Similar behavior was encountered in metallocenium $[MeB(C_6F_5)_3]$ ion pairs,[38] suggesting that the $[D{-}AlO_x]^-$ anions are weakly coordinated to the zirconium deuteride cation in 4-d_2/Al^{i}Bu$_3$/Al_2O_3. At −100 °C, this exchange process is slow on the ^{2}H NMR time scale, and individual signals for $[Cp^b{}_2Zr{-}D][D{-}AlOx]$ in 4-d_2/Al^{i}Bu$_3$/Al_2O_3 are obtained. −100 °C is cold enough to slow the exchange between the active sites in 4-d_2/Al^{i}Bu$_3$/Al_2O_3 but not cold enough to slow rotation in the sp^3 C−D bonds in Al^{i}Bu$_3$/Al_2O_3 ($C_Q \approx$ 170 kHz). The C_Q and η values for the $[Cp^b{}_2Zr{-}D]^+$ fragment in 4-d_2/Al^{i}Bu$_3$/Al_2O_3 are in agreement with the trends observed in the representative molecular zirconium deuterides shown in Figure 4.

The bridging Zr−D−Al in 4-d_2/Al^{i}Bu$_3$/Al_2O_3 is similar to other cationic zirconium hydrides containing bridging Zr−H−E (E = $B(C_6F_5)_3$, $HAlR_2$) in solution.[39−41] In many cases, displacement of the bridging hydride by ethylene is slow relative to chain growth in olefin polymerization reactions in solution.[42−45] DFT studies of $[Cp_2ZrMe][MeAlO_x]$, formed from the reaction of Cp_2ZrMe_2 with fully dehydroxylated alumina, showed that the metallocenium fragment is more weakly coordinated to certain sites on the alumina surface than a typical $[MeB(C_6F_5)_3]$ weakly coordinating anion.[46] This study, and the dynamics of 4-d_2/Al^{i}Bu$_3$/Al_2O_3 from the ^{2}H MAS NMR data reported here, suggests that $[D\text{-}AlO_x]^-$ is also bound more weakly to the $[Cp^b{}_2Zr\text{-}D]^+$ fragment than typical bridging hydrides in solution and is consistent with the high polymerization activity of 4/Al^{i}Bu$_3$/Al_2O_3.

CONCLUSION

The combination of **1**, Al^{i}Bu$_3$, and Al_2O_3 results in active catalysts for the polymerization of ethylene that approach single-site behavior under appropriate conditions. Excess Al^{i}Bu$_3$ is essential in this mixture to rapidly react with the −OH sites on Al_2O_3 and to activate **1** to form **2**.[47] Both of these reactions result in unexpected reaction products that play critical interconnected roles that lead to the formation of active sites in this catalyst. The distribution of $(\equiv AlO)_2Al^iBu(O\text{-}(AlO_x)_2$ present in Al^{i}Bu$_3$/Al_2O_3 are not capable of reacting with **1** to form active sites. This result is surprising given the well-known ability of partially hydrolyzed alkylaluminums to activate metallocene precatalysts in solution.[5] However, the Al−^{i}Bu groups in Al^{i}Bu$_3$/Al_2O_3 are critical because they prevent the reaction of −OH on Al_2O_3 with the zirconium hydrides formed by the reaction of Al^{i}Bu$_3$ and **1**. Passivation of −OH groups on Al_2O_3 with Al^{i}Bu$_3$ allows **2** to react with Lewis sites still present on the passivated Al_2O_3 surface[48,49] and is similar to the reactions of $Cp^*{}_2ThMe_2$ with fully dehydroxylated alumina reported over 35 years ago.[17] The data presented here connects a typical ternary heterogeneous catalyst formulation relevant to industry to well-defined organometallics supported on oxides and homogeneous metallocene catalysts. This understanding gives a simple model to guide catalyst formulations that may result in heterogeneous catalysts for the synthesis of advanced polyolefin materials using a more rational structure−property optimization strategy.

ASSOCIATED CONTENT

Supporting Information

The Supporting Information is available free of charge at https://pubs.acs.org/doi/10.1021/acscentsci.1c00466.

Experimental details, computational details solid-state NMR spectra, FTIR data (PDF)

AUTHOR INFORMATION

Corresponding Authors

Matthew P. Conley − *Department of Chemistry, University of California, Riverside, California 92507, United States;* orcid.org/0000-0001-8593-5814; Email: matthew.conley@ucr.edu

Graham R. Lief − *Bartlesville Research and Technology Center, Chevron Phillips Chemical, Bartlesville, Oklahoma 74003, United States*; Email: liefgr@cpchem.com

Authors

Damien B. Culver − *Department of Chemistry, University of California, Riverside, California 92507, United States;* orcid.org/0000-0001-8294-6059

Rick W. Dorn − *Department of Chemistry, Iowa State University, Ames, Iowa 50011, United States*

Amrit Venkatesh − *Department of Chemistry, Iowa State University, Ames, Iowa 50011, United States;* orcid.org/0000-0001-5319-9269

Jittima Meeprasert − *Inorganic Systems Engineering Group, Department of Chemical Engineering, Faculty of Applied Sciences, Delft University of Technology, Delft 2629 HZ, The Netherlands*

Aaron J. Rossini − *Department of Chemistry, Iowa State University, Ames, Iowa 50011, United States;* orcid.org/0000-0002-1679-9203

Evgeny A. Pidko − *Inorganic Systems Engineering Group, Department of Chemical Engineering, Faculty of Applied Sciences, Delft University of Technology, Delft 2629 HZ, The Netherlands;* orcid.org/0000-0001-9242-9901

Andrew S. Lipton − *Environmental Molecular Sciences Laboratory, Pacific Northwest National Laboratory, Richland, Washington 99354, United States;* orcid.org/0000-0003-4937-4145

Complete contact information is available at: https://pubs.acs.org/10.1021/acscentsci.1c00466

Notes

The authors declare no competing financial interest.

ACKNOWLEDGMENTS

This work was supported by Chevron Phillips Chemical and in part by the National Science Foundation CHE-1800561 (M.P.C). This work was also supported in part from the National Science Foundation CBET-1916809 (R.W.D and A.J.R), the donors of the American Chemical Society Petroleum Research Fund 58627-DNI6 (A.V. and A.J.R), the Sloan Foundation (A.J.R), the European Research Council (ERC) under the European Union's Horizon 2020 research

and innovation programme 725686 (E.A.P), and the Royal Thai Government Scholarships (J.M.). The use of supercomputer facilities for DFT calculations was sponsored by NWO Domain Science. ^{2}H MAS NMR spectra at 18.8 T (−20 °C) were acquired at the MRL Shared Experimental Facilities, which are supported by the MRSEC Program of the NSF (DMR-1720256); a member of the NSF-funded Materials Research Facilities Network. The −100 °C ^{2}H MAS NMR data for 4-d_2/Al^{i}Bu$_3$/Al$_2$O$_3$ was performed using EMSL (grid.436923.9), a DOE Office of Science User Facility sponsored by the Biological and Environmental Research program. We thank Chevron Phillips Chemical for permission to publish this study, and Prof. Kensha M. Clark (University of Memphis) for initiating this project when employed by Chevron Phillips Chemical. M.P.C. is a member of the UCR Center for Catalysis.

REFERENCES

(1) Wilke, G. Fifty Years of Ziegler Catalysts: Consequences and Development of an Invention. *Angew. Chem., Int. Ed.* **2003**, *42*, 5000−5008.
(2) Busico, V. Giulio Natta and the Development of Stereoselective Propene Polymerization. In *Polyolefins: 50 Years after Ziegler and Natta I: Polyethylene and Polypropylene*; Kaminsky, W., Ed.; Springer: Berlin, Heidelberg, 2013; pp 37−57.
(3) Cecchin, G.; Giampiero, M.; Piemontesi, F., Ziegler-Natta Catalysts. In *Kirk-Othmer Encyclopedia of Chemical Technology*; John Wiley & Sons, 2003; Vol. *26*, pp 502−554.
(4) Long, W. P.; Breslow, D. S. Polymerization of Ethylene with Bis-(cyclopentadienyl)-titanium Dichloride and Diethylaluminum Chloride. *J. Am. Chem. Soc.* **1960**, *82*, 1953−1957.
(5) Kaminsky, W. The discovery of metallocene catalysts and their present state of the art. *J. Polym. Sci., Part A: Polym. Chem.* **2004**, *42*, 3911−3921.
(6) Jordan, R. F.; Bajgur, C. S.; Willett, R.; Scott, B. Ethylene Polymerization by a Cationic Dicyclopentadienylzirconium(IV) Alkyl Complex. *J. Am. Chem. Soc.* **1986**, *108*, 7410−7411.
(7) Chen, E. Y.-X.; Marks, T. J. Cocatalysts for Metal-Catalyzed Olefin Polymerization: Activators, Activation Processes, and Structure-Activity Relationships. *Chem. Rev.* **2000**, *100*, 1391−1434.
(8) Bochmann, M. The Chemistry of Catalyst Activation: The Case of Group 4 Polymerization Catalysts. *Organometallics* **2010**, *29*, 4711−4740.
(9) Coates, G. W.; Hustad, P. D.; Reinartz, S. Catalysts for the Living Insertion Polymerization of Alkenes: Access to New Polyolefin Architectures Using Ziegler−Natta Chemistry. *Angew. Chem., Int. Ed.* **2002**, *41*, 2236−2257.
(10) Arriola, D. J.; Carnahan, E. M.; Hustad, P. D.; Kuhlman, R. L.; Wenzel, T. T. Catalytic Production of Olefin Block Copolymers via Chain Shuttling Polymerization. *Science* **2006**, *312*, 714−719.
(11) Eagan, J. M.; Xu, J.; Di Girolamo, R.; Thurber, C. M.; Macosko, C. W.; LaPointe, A. M.; Bates, F. S.; Coates, G. W. Combining polyethylene and polypropylene: Enhanced performance with PE/iPP multiblock polymers. *Science* **2017**, *355*, 814−816.
(12) Severn, J. R.; Chadwick, J. C.; Duchateau, R.; Friederichs, N. Bound but Not Gagged" Immobilizing Single-Site α-Olefin Polymerization Catalysts. *Chem. Rev.* **2005**, *105*, 4073−4147.
(13) Hlatky, G. G. Heterogeneous Single-Site Catalysts for Olefin Polymerization. *Chem. Rev.* **2000**, *100*, 1347−1376.
(14) Ballard, D. G. H. Transition metal alkyl compounds as polymerization catalysts. *J. Polym. Sci., Polym. Chem. Ed.* **1975**, *13*, 2191−2212.
(15) Zakharov, V. A.; Dudchenko, V. K.; Paukshtis, E. A.; Karakchiev, L. G.; Yermakov, Y. I. Formation of zirconium hydrides in supported organozirconium catalysts and their role in ethylene polymerization. *J. Mol. Catal.* **1977**, *2*, 421−435.
(16) Marks, T. J. Surface-bound metal hydrocarbyls. Organometallic connections between heterogeneous and homogeneous catalysis. *Acc. Chem. Res.* **1992**, *25*, 57−65.
(17) Toscano, P. J.; Marks, T. J. Supported organoactinides. High-resolution solid-state carbon-13 NMR studies of catalytically active, alumina-bound pentamethylcyclopentadienyl)thorium methyl and hydride complexes. *J. Am. Chem. Soc.* **1985**, *107*, 653−659.
(18) Jezequel, M.; Dufaud, V. r.; Ruiz-Garcia, M. J.; Carrillo-Hermosilla, F.; Neugebauer, U.; Niccolai, G. P.; Lefebvre, F.; Bayard, F.; Corker, J.; Fiddy, S.; Evans, J.; Broyer, J.-P.; Malinge, J.; Basset, J.-M. Supported Metallocene Catalysts by Surface Organometallic Chemistry. Synthesis, Characterization, and Reactivity in Ethylene Polymerization of Oxide-Supported Mono- and Biscyclopentadienyl Zirconium Alkyl Complexes: Establishment of Structure/Reactivity Relationships. *J. Am. Chem. Soc.* **2001**, *123*, 3520−3540.
(19) Stalzer, M.; Delferro, M.; Marks, T. Supported Single-Site Organometallic Catalysts for the Synthesis of High-Performance Polyolefins. *Catal. Lett.* **2015**, *145*, 3−14.
(20) Wegener, S. L.; Marks, T. J.; Stair, P. C. Design Strategies for the Molecular Level Synthesis of Supported Catalysts. *Acc. Chem. Res.* **2012**, *45*, 206−214.
(21) Copéret, C.; Chabanas, M.; Petroff Saint-Arroman, R.; Basset, J.-M. Homogeneous and Heterogeneous Catalysis: Bridging the Gap through Surface Organometallic Chemistry. *Angew. Chem., Int. Ed.* **2003**, *42*, 156−181.
(22) Copéret, C.; Comas-Vives, A.; Conley, M. P.; Estes, D. P.; Fedorov, A.; Mougel, V.; Nagae, H.; Núñez-Zarur, F.; Zhizhko, P. A. Surface Organometallic and Coordination Chemistry toward Single-Site Heterogeneous Catalysts: Strategies, Methods, Structures, and Activities. *Chem. Rev.* **2016**, *116*, 323−421.
(23) Pelletier, J. D. A.; Basset, J.-M. Catalysis by Design: Well-Defined Single-Site Heterogeneous Catalysts. *Acc. Chem. Res.* **2016**, *49*, 664−677.
(24) McDaniel, M. P.; Jensen, M. D.; Jayaratne, K.; Collins, K. S.; Benham, E. A.; Mcdaniel, N. D.; Das, P. K.; Martin, J. L.; Yang, Q.; Thorn, M. G.; Masino, A. P. Metallocene Activation by Solid Acids. In *Tailor-Made Polymers*; Severn, J. R.; Chadwick, J. C., Eds.; Wiley, 2008; pp 171−210.
(25) For related work using chiral zirconocene dichloride/AlMe$_3$/MAO/Al$_2$O$_3$, see: Collins, S.; Kelly, W. M.; Holden, D. A. Polymerization of propylene using supported, chiral, ansa-metallocene catalysts: production of polypropylene with narrow molecular weight distributions. *Macromolecules* **1992**, *25*, 1780−1785.
(26) Kerber, R. N.; Kermagoret, A.; Callens, E.; Florian, P.; Massiot, D.; Lesage, A.; Copéret, C.; Delbecq, F.; Rozanska, X.; Sautet, P. Nature and Structure of Aluminum Surface Sites Grafted on Silica from a Combination of High-Field Aluminum-27 Solid-State NMR Spectroscopy and First-Principles Calculations. *J. Am. Chem. Soc.* **2012**, *134*, 6767−6775.
(27) Baldwin, S. M.; Bercaw, J. E.; Brintzinger, H. H. Alkylaluminum-Complexed Zirconocene Hydrides: Identification of Hydride-Bridged Species by NMR Spectroscopy. *J. Am. Chem. Soc.* **2008**, *130*, 17423−17433.
(28) Stockland, R. A.; Foley, S. R.; Jordan, R. F. Reaction of vinyl chloride with group 4 metal olefin polymerization catalysts. *J. Am. Chem. Soc.* **2003**, *125*, 796−809.
(29) Stockland, R. A.; Jordan, R. F. Reaction of vinyl chloride with a prototypical metallocene catalyst: Stoichiometric insertion and beta-Cl elimination reactions with rac-(EBI)ZrMe+ and catalytic dechlorination/oligomerization to oligopropylene by rac-(EBI)-ZrMe2/MAO. *J. Am. Chem. Soc.* **2000**, *122*, 6315−6316.
(30) Liu, Z.; Somsook, E.; Landis, C. R. A 2H-Labeling Scheme for Active-Site Counts in Metallocene-Catalyzed Alkene Polymerization. *J. Am. Chem. Soc.* **2001**, *123*, 2915−2916.
(31) Butler, L. G.; Keiter, E. A. Interpretation of Electric Field Gradients at Deuterium as Measured by Solid-State NMR Spectroscopy. *J. Coord. Chem.* **1994**, *32*, 121−134.
(32) Pool, J. A.; Lobkovsky, E.; Chirik, P. J. Cyclopentadienyl Substituent Effects on Reductive Elimination Reactions in Group 4

https://doi.org/10.1021/acscentsci.1c00466
ACS Cent. Sci. 2021, 7, 1225−1231

Metallocenes: Kinetics, Mechanism, and Application to Dinitrogen Activation. *J. Am. Chem. Soc.* **2003**, *125*, 2241−2251.
(33) Pool, J. A.; Bradley, C. A.; Chirik, P. J. A Convenient Method for the Synthesis of Zirconocene Hydrido Chloride, Isobutyl Hydride, and Dihydride Complexes Using tert-Butyl Lithium. *Organometallics* **2002**, *21*, 1271−1277.
(34) McAlister, D. R.; Erwin, D. K.; Bercaw, J. E. Reductive elimination of isobutane from an isobutyl hydride derivative of bis(pentamethylcyclopentadienyl)zirconium. *J. Am. Chem. Soc.* **1978**, *100*, 5966−5968.
(35) Yang, X.; Stern, C. L.; Marks, T. J. Cationic Metallocene Polymerization Catalysts. Synthesis and Properties of the First Base-Free Zirconocene Hydride. *Angew. Chem., Int. Ed. Engl.* **1992**, *31*, 1375−1377.
(36) Jarrett, W. L.; Farlee, R. D.; Butler, L. G. Observation of bridging and terminal metal hydrides by solid-state deuterium NMR spectroscopy: application to bis(cyclopentadienyl)zirconium dideuteride. *Inorg. Chem.* **1987**, *26*, 1381−1383.
(37) $(C_5Me_5)_2ZrD_2$ was synthesized from the reaction of $(C_5Me_5)_2Zr(^iBu)H$ and D_2 (see ref 33). Incorporation of deuterium into the C_5Me_5 ligand is common under these conditions.
(38) Yang, X.; Stern, C. L.; Marks, T. J. Cationic Zirconocene Olefin Polymerization Catalysts Based on the Organo-Lewis Acid Tris-(pentafluorophenyl)borane. A Synthetic,Structural, Solution Dynamic, and Polymerization Catalytic Study. *J. Am. Chem. Soc.* **1994**, *116*, 10015−10031.
(39) Bryliakov, K. P.; Talsi, E. P.; Voskoboynikov, A. Z.; Lancaster, S. J.; Bochmann, M. Formation and Structures of Hafnocene Complexes in MAO- and AlBui3/CPh3[B(C6F5)4]-Activated Systems. *Organometallics* **2008**, *27*, 6333−6342.
(40) Baldwin, S. M.; Bercaw, J. E.; Brintzinger, H. H. Cationic Alkylaluminum-Complexed Zirconocene Hydrides as Participants in Olefin Polymerization Catalysis. *J. Am. Chem. Soc.* **2010**, *132*, 13969−13971.
(41) Baldwin, S. M.; Bercaw, J. E.; Henling, L. M.; Day, M. W.; Brintzinger, H. H. Cationic Alkylaluminum-Complexed Zirconocene Hydrides: NMR-Spectroscopic Identification, Crystallographic Structure Determination, and Interconversion with Other Zirconocene Cations. *J. Am. Chem. Soc.* **2011**, *133*, 1805−1813.
(42) Christianson, M. D.; Tan, E. H. P.; Landis, C. R. Stopped-Flow NMR: Determining the Kinetics of [rac-(C2H4(1-indenyl)2)ZrMe]-[MeB(C6F5)3]-Catalyzed Polymerization of 1-Hexene by Direct Observation. *J. Am. Chem. Soc.* **2010**, *132*, 11461−11463.
(43) Al-Humydi, A.; Garrison, J. C.; Mohammed, M.; Youngs, W. J.; Collins, S. Propene polymerization using ansa-metallocenium ions: Catalyst deactivation processes during monomer consumption and molecular structures of the products formed. *Polyhedron* **2005**, *24*, 1234−1249.
(44) Joshi, A.; Zijlstra, H. S.; Collins, S.; McIndoe, J. S. Catalyst Deactivation Processes during 1-Hexene Polymerization. *ACS Catal.* **2020**, *10*, 7195−7206.
(45) A recent study describes a new activator that appears to avoid bridging hydride formation: Zaccaria, F.; Zuccaccia, C.; Cipullo, R.; Budzelaar, P. H. M.; Vittoria, A.; Macchioni, A.; Busico, V.; Ehm, C. Methylaluminoxane's Molecular Cousin: A Well-defined and "Complete" Al-Activator for Molecular Olefin Polymerization Catalysts. *ACS Catal.* **2021**, *11*, 4464−4475.
(46) Motta, A.; Fragalà, I. L.; Marks, T. J. Links Between Single-Site Heterogeneous and Homogeneous Catalysis. DFT Analysis of Pathways for Organozirconium Catalyst Chemisorptive Activation and Olefin Polymerization on γ-Alumina. *J. Am. Chem. Soc.* **2008**, *130*, 16533−16546.
(47) During the peer-review process, a new study appeared showing that Al^iBu_3 forms hydrides in reactions with supported organometallics: Kanbur, U.; Zang, G.; Paterson, A. L.; Chatterjee, P.; Hackler, R. A.; Delferro, M.; Slowing, I. I.; Perras, F. A.; Sun, P.; Sadow, A. D. Catalytic carbon-carbon bond cleavage and carbon-element bond formation give new life for polyolefins as biodegradable surfactants. *Chem.* **2021**, *7*, 1347−1362.
(48) Joubert, J.; Delbecq, F.; Sautet, P.; Le Roux, E.; Taoufik, M.; Thieuleux, C.; Blanc, F.; Coperet, C.; Thivolle-Cazat, J.; Basset, J.-M. Molecular Understanding of Alumina Supported Single-Site Catalysts by a Combination of Experiment and Theory. *J. Am. Chem. Soc.* **2006**, *128*, 9157−9169.
(49) Wischert, R.; Laurent, P.; Copéret, C.; Delbecq, F.; Sautet, P. Alumina: The Essential and Unexpected Role of Water for the Structure, Stability, and Reactivity of 'Defect' Sites. *J. Am. Chem. Soc.* **2012**, *134*, 14430−14449.

https://doi.org/10.1021/acscentsci.1c00466
ACS Cent. Sci. 2021, 7, 1225−1231